1

The MESSENGER Mission: Science and Implementation Overview

SEAN C. SOLOMON AND BRIAN J. ANDERSON

1.1 INTRODUCTION

Although a sibling of Earth, Venus, and Mars, the planet Mercury is an unusual member of the family (Solomon, 2003). Among the planets of our solar system, it is the smallest, at little more than 5% of an Earth mass, but its bulk density corrected for the effect of internal compression is the highest. Mercury's orbit is the most eccentric of the planets, and it is the only known solar system object in a 3:2 spin–orbit resonance, in which three sidereal days equal two periods of Mercury's revolution about the Sun. Mercury is the only inner planet other than Earth to host an internal magnetic field and an Earth-like magnetosphere capable of standing off the solar wind. The closest planet to the Sun, Mercury experiences a variation in surface temperature at the equator of 600°C over the course of a solar day, which because of Mercury's slow spin rate equals two Mercury years. The permanently shadowed floors of Mercury's high-latitude craters nonetheless are sufficiently cold to have trapped water ice and other frozen volatiles.

Thought to have been created by the same processes as the other inner planets and at the same early stage in the history of the solar system, Mercury with its unusual attributes has long held out the promise of deepening our understanding of how Earth and other Earth-like planets formed and evolved. Yet Mercury is not an easy object to study. Never separated from the Sun by more than 28° of arc when viewed from Earth, Mercury is forbidden as a target for the Hubble Space Telescope and other astronomical facilities because their optical systems would be severely damaged by exposure to direct sunlight. Located deep within the gravitational potential well of the Sun, Mercury has also long presented a challenge to spacecraft mission design. The first spacecraft to view Mercury at close range was Mariner 10, which after flying once by Venus encountered the innermost planet three times in 1974–1975. The encounters occurred nearly at Mercury's greatest distance from the Sun and were spaced approximately one Mercury solar day apart, so the same hemisphere of the planet was in sunlight at each flyby. Mariner 10 obtained images of 45% of the surface, discovered the planet's global magnetic field, assayed three neutral species (H, He, and O) in Mercury's tenuous atmosphere, and sampled the magnetic field and energetic charged particles in Mercury's dynamic magnetosphere (Dunne and Burgess, 1978).

After the Mariner 10 mission, the next logical step in the exploration of Mercury was widely viewed to be an orbiter mission (COMPLEX, 1978), and several notable discoveries by ground-based astronomers in the years since the Mariner 10 encounters (e.g., Potter and Morgan, 1985, 1986; Slade et al., 1992; Harmon and Slade, 1992) provided a wealth of new information about Mercury that whetted the appetite of the planetary science community for orbital observations. Nevertheless, substantial advances were needed in mission design, thermal engineering, and miniaturization of instruments and spacecraft subsystems before such a mission could be considered technically ready.

The MErcury Surface, Space ENvironment, GEochemistry, and Ranging (MESSENGER) mission to orbit Mercury was proposed under NASA's Discovery Program in 1996 and again in 1998 (Solomon et al., 2001; Gold et al., 2001; Santo et al., 2001) and was selected for flight in 1999. Development, construction, integration, and testing of the spacecraft and its instruments began in January 2000 and spanned the four and a half years leading to launch on 3 August 2004 (McNutt et al., 2006). MESSENGER completed gravity-assist flybys of Earth once, Venus twice, and Mercury three times (Figure 1.1) during a mission cruise phase that lasted 6.6 years. MESSENGER was inserted into orbit about Mercury on 18 March 2011 and conducted orbital observations of the innermost planet for more than four years, until 30 April 2015.

In this chapter we provide an overview of the MESSENGER mission from a historical perspective, including the mission's scientific objectives; the payload characteristics, data acquisition planning, and operational procedures adopted to achieve those objectives; and the scientific findings from flyby and orbital operations. We begin with summaries of the mission objectives, spacecraft, payload instruments, and orbit design. We then describe the procedures adopted to optimize the scientific return from the complex series of orbital data acquisition operations. We follow with an account of the primary mission, including the Mercury flybys and the first year of orbital observations. We then outline the rationale for and accomplishments of MESSENGER's first extended mission, conducted over the second year of orbital operations, and the second extended mission, conducted over the final two years of orbital operations. The second extended mission included a distinctive low-altitude campaign completed at the culmination of the mission. A concluding section briefly introduces the other chapters of this book.

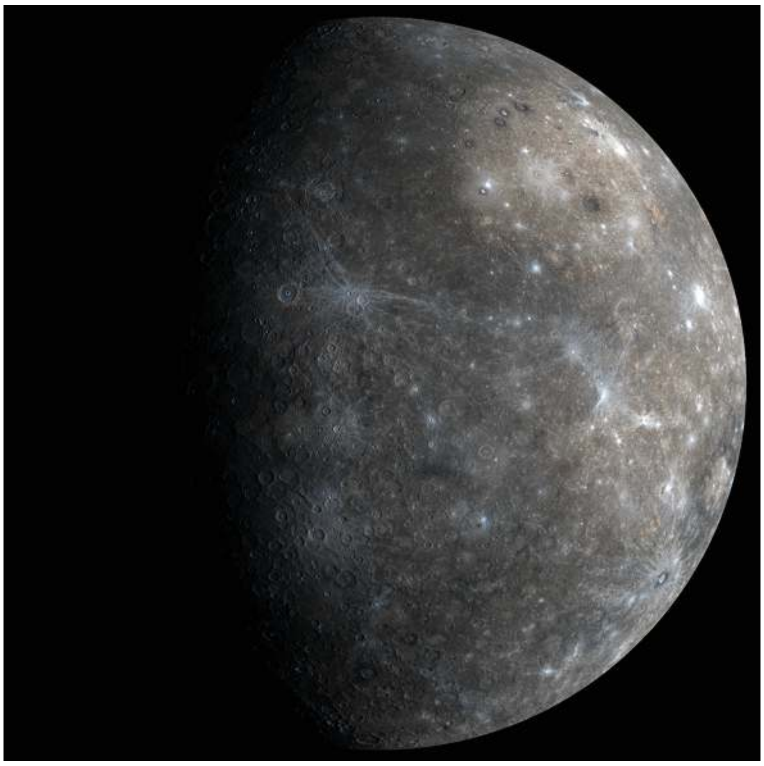

Figure 1.1. Image mosaic of Mercury acquired on departure from MESSENGER's first Mercury flyby on 14 January 2008. Mercury Dual Imaging System wide-angle camera images acquired through the narrow-band filters centered at 1000, 700, and 430 nm are projected in red, green, and blue in this color representation. Much of the area shown had not been imaged by Mariner 10.

1.2 MISSION OBJECTIVES, SPACECRAFT, PAYLOAD, AND ORBIT DESIGN

1.2.1 Key Scientific Questions

The MESSENGER mission was designed to address six key scientific questions. The questions were motivated by the knowledge of Mercury available at the time the mission was proposed, were capable of being substantially addressed by measurements that could be made from orbit, and would yield answers that would bear not only on the nature of Mercury but more generally on the origin and comparative evolution of the inner planets as a group. Those questions and a brief summary of the rationale for each were as follows.

1.2.1.1 What Planetary Formational Processes Led to the High Ratio of Metal to Silicate in Mercury?

The Mariner 10 spacecraft carried no elemental remote sensing instruments, so at the time the MESSENGER mission was proposed the single most important piece of information about the planet's bulk composition was its high uncompressed density, which implied that Mercury has an iron-rich core that occupies much higher fractions of the planet's mass and volume than do the cores of the other inner planets (e.g., Siegfried and Solomon, 1974). A variety of theories for the origin and early evolution of Mercury had been advanced to account for its high metal fraction, including formation from metal-enriched precursors resulting from either high-temperature fractionation or aerodynamical sorting in the solar nebula (e.g., Weidenschilling, 1978; Lewis, 1988) or removal of an initially larger silicate crust and mantle by evaporation or giant impact (e.g., Cameron, 1985; Wetherill, 1988; Benz et al., 1988). Those theories differed in their predictions for the bulk composition of the silicate fraction of the planet (e.g., Lewis, 1988), including the upper crust, which would be visible to geochemical remote sensing instruments on an orbiting spacecraft. Moreover, ground-based telescopic measurements of Mercury's surface reflectance showed few if any absorption features commonly seen in reflectance spectra of the Moon, Mars, and asteroids and attributable to the presence of ferrous iron in silicate minerals (e.g., Vilas, 1988), indicating both a low abundance of ferrous iron on Mercury's surface and the need to rely heavily on elemental remote sensing instruments to gain compositional information.

1.2.1.2 What Is the Geological History of Mercury?

Because of Mercury's size, intermediate between the Moon and Mars, as well as its high metal/silicate ratio, documenting the geological history of Mercury was viewed as crucial to understanding how terrestrial planet evolution depends on planet size and initial conditions. A broad geological history of Mercury had been developed from Mariner 10 images (e.g., Strom, 1979; Spudis and Guest, 1988), but the limited coverage and resolution of those images left many aspects of that history uncertain. Extensive plains units were documented by Mariner 10, and the youngest of those plains deposits were seen to be in stratigraphic positions similar to the volcanic lunar maria. Unlike the maria, however, the plains deposits on Mercury are not markedly lower in reflectance than the surrounding older terrain, and no volcanic landforms were visible at the resolution of Mariner 10 images, so both volcanic and impact ejecta processes for plains emplacement had been suggested (e.g., Strom et al., 1975; Wilhelms,

1976) and the importance of volcanism in Mercury's history was thus uncertain. Deformational features on Mercury were seen to be dominantly contractional, leading to the proposal that such features were the expression of global contraction resulting from interior cooling (e.g., Strom et al., 1975), although the restricted imaging coverage meant that the global contraction hypothesis remained untested over slightly more than a full hemisphere of the planet.

1.2.1.3 What Are the Nature and Origin of Mercury's Magnetic Field?

Measurements by Mariner 10 demonstrated that Mercury has an internal magnetic field (Ness et al., 1976) with a dipole component nearly orthogonal to the planet's orbital plane and an estimated moment near 300 nT $R_M{}^3$, where R_M is Mercury's mean radius (Connerney and Ness, 1988). Because external sources can dominate the total field measured at Mercury, and because of the limited sampling of the field during the two Mariner 10 flybys that penetrated Mercury's magnetosphere, the uncertainty in Mercury's dipole moment derived from Mariner 10 data was a factor of 2, and higher-order terms were linearly dependent and thus not resolvable (Connerney and Ness, 1988). A variety of mechanisms for producing Mercury's observed magnetic field had been proposed, including remanent or fossil fields in Mercury's crust and lithosphere (Stephenson, 1976; Srnka, 1976; Aharonson et al., 2004), hydromagnetic dynamos in a fluid outer core (e.g., Schubert et al., 1988; Stanley et al., 2005; Christensen, 2006), and a thermoelectric dynamo driven by temperature differences along the top of the core (Stevenson, 1987; Giampieri and Balogh, 2002). The different field generation models made different predictions regarding the geometry of the field, particularly for terms of higher order than the dipole term, and so measurements made from orbit about the planet were seen to be needed to distinguish among hypotheses.

1.2.1.4 What Are the Structure and State of Mercury's Core?

The size and physical state of Mercury's core are key to understanding the planet's bulk composition, thermal history, and magnetic field generation processes (Zuber et al., 2007). Peale (1976) realized that the existence and radius of a liquid outer core on Mercury can be determined by the measurement of Mercury's obliquity, the amplitude of its physical libration forced by variations in the torque exerted by the gravitational pull of the Sun over the planet's 88-day orbit period, and two quantities that define the shape of the planet's gravity field at spherical harmonic degree and order 2. The required coefficients in the spherical harmonic expansion of Mercury's gravity field had been estimated from radio tracking of the Mariner 10 flybys (Anderson et al., 1987) but not with high precision. All four quantities can be determined from measurements made by an orbiting spacecraft with sufficient precision to determine Mercury's polar moment of inertia and the moment of inertia of the planet's solid outer shell that participates in the 88-day libration (Peale, 1976: Peale et al., 2002), and from those quantities important aspects of Mercury's internal structure can be resolved. Mercury's obliquity and forced libration amplitude can also be measured from Earth-based radar observations, and such measurements were reported by Margot et al. (2007) before MESSENGER was inserted into orbit around Mercury, and then refined several years later (Margot et al., 2012). Although the measurements of libration amplitude and obliquity indicated that Mercury does indeed possess a fluid outer core (Margot et al., 2007), the uncertainties in Mercury's gravitational field coefficients at harmonic degree 2 dominated the uncertainty in the planet's moments of inertia. Radio tracking of an orbiting spacecraft was required to improve the determination of these key quantities.

1.2.1.5 What Are the Radar-Reflective Materials at Mercury's Poles?

The discovery in 1991 of radar-bright regions near Mercury's poles and the similarity of the radar reflectivity and polarization characteristics of such regions to those of icy satellites and the south residual polar cap of Mars led to the proposal that these areas host deposits of surface or near-surface water ice (Slade et al., 1992; Harmon and Slade, 1992). Subsequent radar imaging at improved resolution confirmed that the radar-bright deposits are confined to the floors of near-polar impact craters (e.g., Harmon et al., 2011). Because of Mercury's small obliquity, sufficiently deep craters are permanently shadowed and are predicted to be at temperatures at which water ice is stable for billions of years (Paige et al., 1992). Although a contribution from interior outgassing could not be excluded, impact volatilization of cometary and meteoritic material followed by transport of water molecules to polar cold traps was shown to provide sufficient polar ice to match the characteristics of the deposits (Moses et al., 1999).

Two alternative explanations for the radar-bright polar deposits of Mercury were nonetheless suggested. One was that the polar deposits are composed of elemental sulfur, on the grounds that sulfur would be stable in polar cold traps and the presence of sulfides in the regolith can account for a high disk-averaged index of refraction and low microwave opacity of surface materials (Sprague et al., 1995). The second was that the permanently shadowed portions of polar craters are radar-bright not because of trapped volatiles but because of either unusual surface roughness (Weidenschilling, 1998) or low dielectric loss (Starukhina, 2001) of near-surface silicates at extremely cold temperatures. Geochemical remote sensing measurements made from orbit around Mercury were recognized as able to distinguish among the competing proposals.

1.2.1.6 What Are the Important Volatile Species and Their Sources and Sinks on and near Mercury?

Mercury's atmosphere is a surface-bounded exosphere for which the composition and behavior are controlled by interactions with the magnetosphere and the surface. At the time the MESSENGER mission was under development, the atmosphere was known to contain at least six elements (H, He, O, Na, K, Ca). The Mariner 10 airglow spectrometer detected H and He and set an upper bound on O (Broadfoot et al., 1976), and ground-based spectroscopic observations led to the discovery of exospheric Na (Potter and Morgan, 1985), K (Potter and Morgan, 1986), and Ca (Bida et al., 2000). Exospheric H and He were thought to be dominated by solar wind ions neutralized by recombination at the surface, whereas proposed source processes for other exospheric species included diffusion from the planet's interior, evaporation, sputtering by photons and energetic ions, chemical sputtering by protons, and meteoroid impact and vaporization (e.g., Killen and Ip, 1999). That several of these processes play some role was suggested by the strong variations in exospheric characteristics observed as functions of local time, solar distance, and level of solar activity (e.g., Sprague et al., 1998; Hunten and Sprague, 2002; Leblanc and Johnson, 2003). It was long recognized that a spacecraft in orbit about Mercury can provide a range of opportunities for elucidating further the nature of the exosphere, through profiles of major exospheric neutral species versus time of day and solar distance and searches for new species (e.g., Domingue et al., 2007). In situ measurement of energetic and thermal plasma ions from orbit can also detect solar wind pickup ions that originated as exospheric neutral atoms (e.g., Koehn et al., 2002).

1.2.2 Scientific Objectives

The six key questions above led to a set of scientific objectives for the MESSENGER mission and in turn to a set of project requirements (Solomon et al., 2001), a suite of payload instruments (Gold et al., 2001), and a measurement strategy (Section 1.3). The scientific objectives for MESSENGER's primary mission are given in Table 1.1, and the project requirements for the primary mission are given in Table 1.2.

The objective to characterize the chemical composition of Mercury's surface led to a project requirement for global maps of major element composition at a resolution sufficient to discern the principal geological units and to distinguish material excavated and ejected by young impact craters from a possible veneer of cometary and meteoritic material. Information on surface mineralogy was also deemed important for this objective. The objective to determine the planet's geological history led to a project requirement for global monochrome imaging at a resolution of hundreds of meters or better, for topographic profiles across key geological features from altimetry or stereo, and for spectral measurements of major geologic units at spatial resolutions of several kilometers or better. The objective to characterize Mercury's magnetic field led to a project requirement for magnetometry, both near the planet and throughout the magnetosphere, as well as for energetic particle and plasma measurements so as to assist in the separation of external and internal fields. The objective to estimate the size and state of Mercury's core led to the project requirement for altimetric measurement of the amplitude of Mercury's physical libration as well as determination of the planet's obliquity and low-degree gravitational field. The objective to assay the volatile inventory at Mercury's poles led to the project requirement for ultraviolet spectrometry of the polar atmosphere and for gamma-ray and neutron spectrometry, imaging, and altimetry of polar-region craters. The objective to characterize the nature of Mercury's exosphere and magnetosphere led to the project requirement to identify all major neutral species in the exosphere and charged species in the magnetosphere.

Table 1.1. *Scientific objectives for MESSENGER's primary mission.*

1. Determine the chemical composition of Mercury's surface.
2. Determine Mercury's geological history.
3. Determine the nature of Mercury's magnetic field.
4. Determine the size and state of Mercury's core.
5. Determine the volatile inventory at Mercury's poles.
6. Determine the nature of Mercury's exosphere and magnetosphere.

1.2.3 Spacecraft

The design of the MESSENGER spacecraft (Figure 1.2) was driven largely by two requirements: to minimize mass and to survive the harsh thermal environment at Mercury (Santo et al., 2001; Leary et al., 2007). The largest launch vehicle available to the Discovery Program was the Delta II 7925-H, which could inject ~1100 kg into the required interplanetary trajectory. Because more than half of that total launch mass was needed for the propellant required to achieve the mission design, only 500 kg remained for the total spacecraft dry mass. To meet this constraint, the spacecraft structure was fabricated primarily with lightweight composite material and was fully integrated with a dual-mode propulsion system that

Table 1.2. *Project requirements for MESSENGER's primary mission.*

1. Provide major-element maps of Mercury to 10% relative uncertainty on the 1000-km scale and determine local composition and mineralogy at the ~20-km scale.
2a. Provide a global map with >90% coverage (monochrome) at 250-m average resolution and >80% of the planet imaged stereoscopically.
2b. Provide a global multispectral map at 2-km/pixel average resolution.
2c. Sample half of the northern hemisphere for topography at 1.5-m average height resolution.
3. Provide a multipole magnetic field model resolved through quadrupole terms with an uncertainty of less than ~20% in the dipole magnitude and direction.
4. Provide a global gravity field to degree and order 16 and determine the ratio of the solid-planet moment of inertia to the total moment of inertia to ~20% or better.
5. Identify the principal component of the radar-reflective material at Mercury's north pole.
6. Provide altitude profiles at 25-km resolution of the major neutral exospheric species and characterize the major ion-species energy distributions as functions of local time, Mercury heliocentric distance, and solar activity.

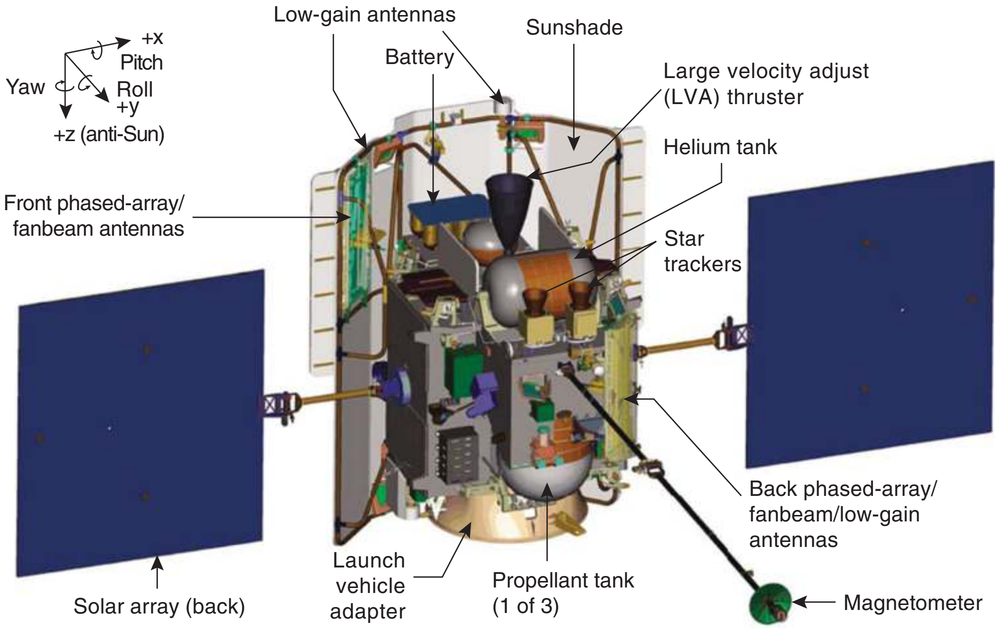

Figure 1.2. Engineering view of the MESSENGER spacecraft from behind the sunshade.

featured lightweight tanks for propellant (hydrazine), oxidizer (nitrous tetroxide), and pressurant (gaseous helium). The propulsion system included a total of 17 thrusters: a single large velocity adjustment bipropellant thruster; four 22-N monopropellant thrusters for thrust-vector steering during large spacecraft maneuvers and for trajectory-correction maneuvers; and 12 4.4-N monopropellant thrusters for attitude control, angular momentum management, and small trajectory-correction maneuvers.

A large number of mass-reduction measures were used in the development of the spacecraft. To avoid a cumbersome gimbaled antenna and the challenges associated with testing and operating it at high temperatures, an electronically steerable phased-array system was developed for the high-gain antenna. Used one at a time, each of two antennas – one on the spacecraft's Sun-facing side and one aft – could be steered about one axis while the spacecraft body rolled about a second axis to point the antenna toward Earth at any point in the mission. The phased-array antennas were complemented with two medium-gain fanbeam antennas and four low-gain antennas. Radio signals were transmitted to and received from the MESSENGER spacecraft at X-band frequencies (7.2-GHz uplink, 8.4-GHz downlink) by the 34-m and 70-m antennas at NASA's Deep Space Network stations in Goldstone, California; Madrid, Spain; and Canberra, Australia.

Mass was also conserved by limiting the number of spacecraft components that moved. With the lone exception of the imaging system (see next section), all science instruments were hard-mounted to the spacecraft. As a consequence, spacecraft attitude often had to be changed continuously in orbit about Mercury to permit the instruments to make their observations.

Spacecraft power was provided by two solar arrays (Figures 1.2 and 1.3), which could be articulated to manage array temperature, and by a battery during those orbits when the spacecraft was on Mercury's nightside and the Sun was eclipsed. In a fully redundant electronics system, a main processor performed all nominal spacecraft functions, while two other processors monitored spacecraft health and safety. The spacecraft attitude control system was three-axis stable and momentum biased and made use of four reaction wheels. Attitude knowledge was acquired through an inertial measurement unit, two star trackers, and a suite of Sun sensors as a backup to the primary attitude sensors.

Primarily passive thermal management techniques were used to minimize heating of spacecraft subsystems by the Sun and the dayside surface of Mercury. To protect the spacecraft from solar heating, all systems except the solar arrays were kept behind a ceramic-cloth sunshade that pointed toward the Sun. This approach simplified the design of the subsystems, which could be built with conventional electronics, but added a substantial constraint to the operation of the spacecraft. Throughout its time within the inner solar system and in orbit about Mercury, MESSENGER was constrained to maintain the orientation of the normal to the central sunshade panel in the sunward direction to within ±10° in Sun-relative elevation angle (pitch) and ±12° in Sun-relative azimuth (yaw) at all times.

1.2.4 Instrument Payload

The project requirements for MESSENGER's primary mission were met by a suite of seven scientific instruments plus the spacecraft communication system (Gold et al., 2001). There was a dual imaging system for wide and narrow fields of view, monochrome and color imaging, and stereo; gamma-ray, neutron, and X-ray spectrometers for surface chemical mapping; a magnetometer; a laser altimeter; a combined ultraviolet–visible and visible–near-infrared spectrometer to survey both exospheric species and surface mineralogy; and a combined energetic particle and plasma spectrometer to

Figure 1.3. View of the MESSENGER spacecraft during vibration testing at the Johns Hopkins University Applied Physics Laboratory. The solar arrays (mirrored surfaces) are stowed in their positions at the time of launch. Also visible are the Magnetometer boom (center), similarly in its stowed position, and thermal blankets (gold).

sample charged species in the magnetosphere (Figure 1.4). Brief descriptions of the payload instruments are as follows.

1.2.4.1 Mercury Dual Imaging System

The Mercury Dual Imaging System (MDIS) on the MESSENGER spacecraft (Hawkins et al., 2007), shown in Figure 1.4, consisted of a monochrome narrow-angle camera (NAC) and a multispectral wide-angle camera (WAC). The NAC was an off-axis reflector with a 1.5° field of view (FOV) and was co-aligned with the WAC, a four-element refractor with a 10.5° FOV and a 12-color filter wheel. The focal-plane electronics of each camera were identical and used a 1024 × 1024 charge-coupled-device detector. Only one camera operated at a time, a design that allowed them to share a common set of control electronics. The NAC and the WAC were mounted on a pivoting platform that provided a 90° field of regard, from 40° sunward to 50° anti-sunward from the spacecraft *z*-axis (Figure 1.2) – the boresight direction of most of MESSENGER's instruments. Onboard data compression provided capabilities for pixel binning, remapping of 12-bit data to 8 bits, and lossless or lossy compression. During MESSENGER's primary mission, four main MDIS data sets were planned: a monochrome global image mosaic at near-zero emission angles and moderate incidence angles, a stereo complement map at off-nadir geometry and near-identical lighting, multicolor images at low incidence angles, and targeted high-resolution images of key surface features. It was further planned that those data would be used to construct a global image base map, a digital terrain model, global maps of color properties, and mosaics of high-resolution image strips.

1.2.4.2 Gamma-Ray and Neutron Spectrometer

The Gamma-Ray and Neutron Spectrometer (GRNS) instrument (Figure 1.4) included separate Gamma-Ray Spectrometer (GRS) and Neutron Spectrometer (NS) sensors (Goldsten et al., 2007). The GRS detector was a mechanically cooled crystal of germanium, and the sensor detected gamma-ray emissions in the energy range 0.1–10 MeV and achieved an energy resolution of 3.5 keV full width at half maximum for ^{60}Co (1332 keV). Special construction techniques provided the necessary thermal isolation to

Cambridge University Press
978-1-107-15445-2 — Mercury
Edited by Sean C. Solomon , Larry R. Nittler , Brian J. Anderson
Excerpt
More Information

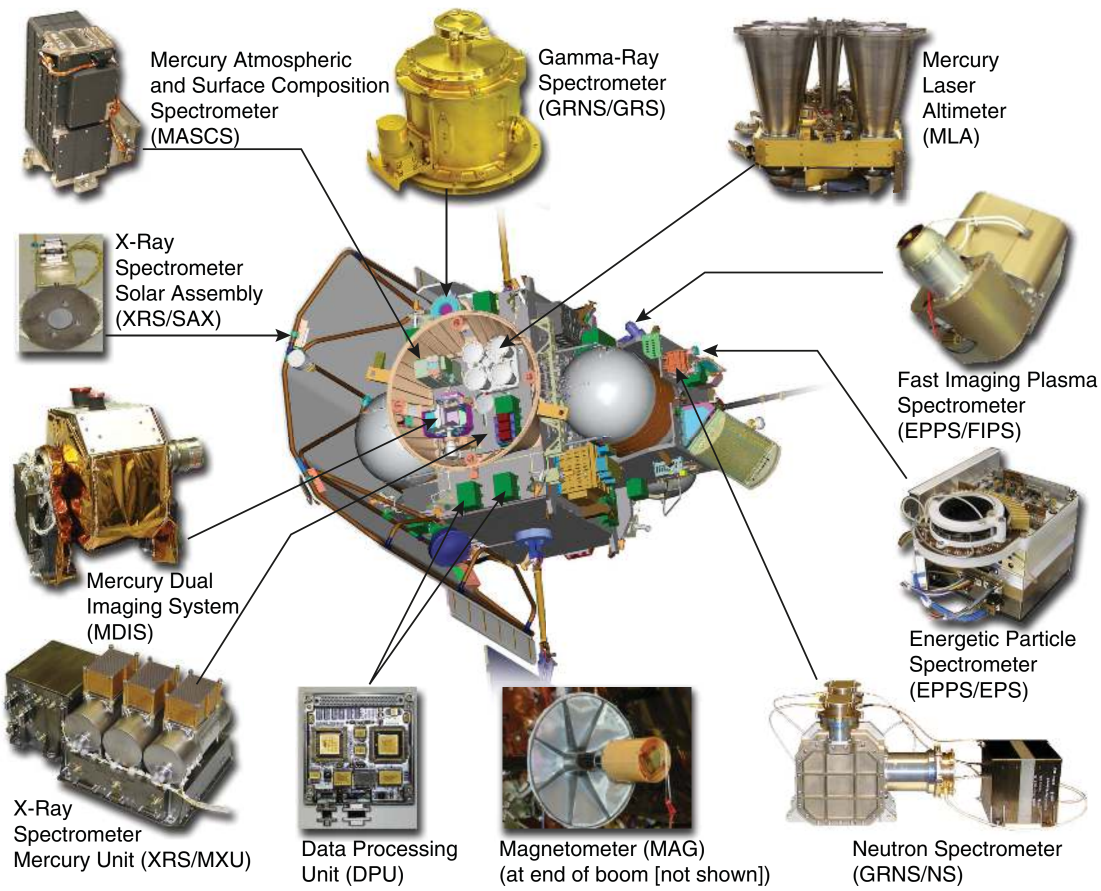

Figure 1.4. MESSENGER instruments and their locations on the spacecraft.

maintain the encapsulated detector at cryogenic temperatures (90 K) despite the high temperatures in Mercury's environment. The outer housing of the GRS sensor was equipped with an anticoincidence shield (ACS) to reduce the background from charged particles. The NS sensor consisted of a sandwich of three scintillation detectors working in concert to measure the flux of neutrons in three energy ranges from thermal to ~7 MeV.

1.2.4.3 X-Ray Spectrometer

The X-Ray Spectrometer (XRS) (Figure 1.4) measured the characteristic X-ray emissions induced on the surface of Mercury by the incident solar X-ray flux (Schlemm et al., 2007). The instrument detected the Kα lines for the elements Mg, Al, Si, S, Ca, Ti, Cr, Mn, and Fe. The planet-viewing sensor (Mercury X-ray Unit, MXU) consisted of three gas-filled proportional counters, one with a thin Mg foil over the entrance window, one with a thin Al foil over the entrance window, and one with no foil to separate the lower-energy lines from Mg, Al, and Si. The 12° field of view of the planet-viewing sensor allowed a spatial resolution that ranged from 42 km at 200-km altitude to 3200 km at 15,000-km altitude. A small Si-PIN detector (Solar Assembly for X-rays, SAX) mounted on the spacecraft sunshade (Leary et al., 2007) and directed sunward provided simultaneous measurement of the solar X-ray flux. The solar detector included a thermoelectric cooler that could also operate in a heater mode to anneal the sensor after radiation damage.

1.2.4.4 Magnetometer

MESSENGER's Magnetometer (MAG) was a low-noise, triaxial fluxgate instrument (Anderson et al., 2007). Its sensor was mounted on a 3.6-m-long boom that was directed generally anti-sunward (Figures 1.2 and 1.3). The instrument had both a coarse range, ±51,300 nT full scale (1.6-nT resolution), for preflight testing, and a fine range, ±1530 nT full scale (0.047-nT resolution), for operation near Mercury. A magnetic cleanliness program followed during the design and construction of the spacecraft minimized variable and static spacecraft-generated fields at the sensor. Analog signals from the three instrument axes were low-pass filtered (10-Hz cutoff) and sampled simultaneously by three 20-bit analog-to-digital converters every 50 ms. To accommodate variable telemetry rates, MAG provided 11 output rates from 0.01 s^{-1} to 20 s^{-1}. The instrument also provided continuous measurement of fluctuations by means of a digital 1–10-Hz bandpass filter. This fluctuation level was used to trigger high-time-resolution sampling in 8-min segments to record events of interest when continuous high-rate sampling was not possible.

1.2.4.5 Mercury Laser Altimeter

The Mercury Laser Altimeter (MLA) (Cavanaugh et al., 2007) (Figure 1.4) measured the round-trip time of flight of transmitted laser pulses reflected from the surface of Mercury which, in combination with the spacecraft orbit position and pointing data, gave a high-precision measurement of surface topography referenced to Mercury's center of mass. The laser transmitter was a diode-pumped Nd:YAG slab laser with passive Q-switching. The transmitter emitted 5-ns-wide pulses at an 8-Hz rate with 20 mJ of energy at a near-infrared wavelength of 1064 nm. The receiver consisted of four refractive telescopes and four equal-length optical fibers to couple the received optical signal onto a single silicon avalanche photodiode. The timing of laser pulses was measured with a set of time-to-digital converters and counters and a crystal oscillator operating at a frequency that was monitored regularly from Earth. MLA sampled the planet's surface to within a 1-m range error when the line-of-sight range to Mercury was less than 1500 km under spacecraft nadir pointing or the slant range was less than ~1000 km at off-nadir angles up to ~40°.

1.2.4.6 Mercury Atmospheric and Surface Composition Spectrometer

MESSENGER's Mercury Atmospheric and Surface Composition Spectrometer (MASCS) (McClintock and Lankton, 2007) consisted of a small Cassegrain telescope with 257-mm effective focal length and a 50-mm aperture that simultaneously fed an Ultraviolet and Visible Spectrometer (UVVS) and a Visible and Infrared Spectrograph (VIRS) (Figure 1.4). UVVS was a 125-mm-focal-length, scanning grating, Ebert–Fastie monochromator equipped with three photomultiplier tube detectors that covered far-ultraviolet (115–180 nm), middle-ultraviolet (160–320 nm), and visible (250–600 nm) wavelength ranges with an average spectral resolution of 0.6 nm. It was designed to measure profiles with altitude of known exospheric species, to search for previously undetected exospheric species, and to observe Mercury's surface in the far and middle ultraviolet at a spatial scale of 10 km or smaller. VIRS was a fixed concave grating spectrograph with a 210-mm focal length equipped with a beam splitter that simultaneously dispersed the spectrum onto a 512-element silicon visible-wavelength photodiode array (300–1050 nm) and a 256-element indium-gallium-arsenide infrared-wavelength photodiode array (850–1450 nm). The VIRS was designed to map surface reflectance with 5-nm spectral resolution in the wavelength range 300–1450 nm.

1.2.4.7 Energetic Particle and Plasma Spectrometer

The Energetic Particle and Plasma Spectrometer (EPPS) instrument on MESSENGER consisted of two sensors (Andrews et al., 2007), an Energetic Particle Spectrometer (EPS) and a Fast Imaging Plasma Spectrometer (FIPS) (Figure 1.4). The EPS was a hockey-puck-sized energy by time-of-flight spectrometer designed to measure in situ the energy, angular, and compositional distributions of the high-energy components of electrons (>20 keV) and ions (>5 keV/nucleon) near Mercury. The FIPS measured the energy, angular, and compositional distributions of the low-energy components of the ion distributions (<50 eV/charge to 20 keV/charge). The FIPS sensor featured an electrostatic analyzer system with a large (1.4 sr) instantaneous field of view.

1.2.4.8 Radio Science

The MESSENGER telecommunications subsystem was designed primarily to send commands to the spacecraft and to transmit to Earth both science measurements and information on the state of the spacecraft and instruments (Srinivasan et al., 2007). The subsystem doubled as a scientific tool by providing precise measurements of the spacecraft's velocity and range along the line of sight to Earth, information essential for spacecraft navigation and also for deriving Mercury's gravity field.

1.2.5 Orbit Design

The parameters selected for the MESSENGER orbit after the orbit insertion maneuver resulted from a complex trade-off of scientific objectives, spacecraft and instrument thermal design, communications and power constraints, and propellant budget (Santo et al., 2001). The original design for the initial orbit featured a periapsis altitude of 200 km, a periapsis latitude of 60°N, an inclination of 80° to the planet's equatorial plane, and a period of 12 h. The periapsis latitude and altitude, the high eccentricity of the orbit, and the phasing of the initial orbit relative to local time and Mercury true anomaly were all selected as part of the mission thermal design. The 12-h period was chosen to regularize the schedule of mission operations and permitted ample time for data downlink near apoapsis.

Orbit-correction maneuvers (OCMs) were planned for the orbital phase of the primary mission, because the gravitational pull of the Sun would raise periapsis altitude and latitude between successive orbits (McAdams et al., 2007). Such maneuvers were planned in pairs, with the first designed to lower periapsis altitude back to ~200 km and the second to adjust the orbit period after the first correction back to 12 h. The pairs of maneuvers were scheduled approximately one Mercury year apart in order to keep periapsis altitude below 500 km while meeting spacecraft sunshade pointing and science requirements.

1.3 MESSENGER'S SCIENCE DATA ACQUISITION PLANNING AND OPERATIONS

Planning for MESSENGER's scientific observations from orbit about Mercury required a novel approach to the design of payload operations and spacecraft attitude-control commanding. Experience with science planning for the Mercury flybys demonstrated the complex interplay between imaging and competing remote sensing observations, as well as with spacecraft operational constraints on pointing, power management, navigation, and achievable rates of change to spacecraft attitude. Planning for the flybys was conducted with conventional manual approaches to the design of observation and spacecraft command sequences with computational and visualization tools. Months of iterative, labor-intensive work were required to design, simulate, and review each encounter. The complexities of operations from orbit about Mercury, however, called for a marked change in the planning architecture, given that the orbital phase of the primary mission phase would be equivalent to two flybys every Earth day. To effect such a change, the observational requirements, spacecraft capabilities, and operational constraints had to be captured in carefully implemented software, which was then used together with orbit solutions in an automated search for optimal observation opportunities and spacecraft attitude, imaging pivot commanding, and instrument commanding. Those objectives were accomplished with a sophisticated, integrated suite of modules known as SciBox (Anderson et al., 2011b; Choo et al., 2014).

1.3.1 Science Observation Constraints

The observational opportunities at Mercury were highly constrained by MESSENGER's eccentric orbit and Mercury's low spin rate. A solar day on Mercury is approximately 176 Earth days, so during MESSENGER's year-long primary orbital mission there were only two opportunities to observe each longitude at a given solar illumination. In addition, the different science investigations had distinct and competing pointing requirements. For monochrome surface imaging, for instance, a specific range of solar incidence angles is optimal to reveal surface features while not obscuring terrain in shadow, whereas for color imaging near-normal solar incidence angles are best. Imaging plans also had to incorporate a favorable phase angle to minimize forward scattering of sunlight yet maintain surface resolution. Moreover, the choice of MDIS camera, wide-angle or narrow-angle, depended on altitude and viewing geometry as well as the need to balance resolution with the requirement to obtain as complete and overlapping imaging coverage as possible.

MESSENGER's other science investigations imposed still different requirements. Most of the instruments on the spacecraft's main instrument deck (Figure 1.4) had co-aligned fields of view and yielded optimal data for near-nadir viewing directions. In contrast, exospheric observations by the UVVS required turning the spacecraft so that the spacecraft z-axis, i.e., the normal to the instrument deck, pointed off the limb of the planet. The MLA observations yielded the highest signal-to-noise ratio for surfaces in darkness, whereas the XRS observations required that the surface be in daylight so as to be exposed to solar X-rays. The GRS observations were largely insensitive to surface illumination, but the NS observations were optimal for specific orientations of the NS detectors with respect to the spacecraft orbital velocity relative to Mercury. Finally, the EPS instrument yielded the most scientifically fruitful data when the magnetic field direction lay in the plane of the instrument field of view.

1.3.2 Spacecraft and Mission Operations Constraints

Over and above the scientific objectives and instrument observational constraints, ensuring the continued health of the spacecraft and payload demanded attention to spacecraft operations, communications, and navigation considerations. The constraints on spacecraft attitude were strictly enforced to maintain the orientation of the normal to the central sunshade panel in the direction of the Sun to within specified tolerances in the Sun-relative elevation angle and azimuth. Violation of these constraints would trigger autonomous spacecraft protection procedures and abort the science observation sequence, so the planning software imposed these constraints as hard limits on the commanded attitude. Communication passes for command uplink and data downlink and spacecraft angular momentum management were carefully planned and reserved for mission operations. Software tools were developed to allocate spacecraft resources, particularly the solid-state recorder (SSR), to track and predict the onboard data volume against the observation plan to ensure the return to Earth of all collected data. Orbit-adjustment maneuvers and other mission-critical activities were also strictly reserved for mission operations planning and treated as unavailable for science observations that required attitude commanding. Passive science data collection continued through communications operations.

1.3.3 Automated Science Opportunity Analyzer and Scheduler

The MESSENGER SciBox suite of software modules was designed to factor in the payload constraints and priorities for observation geometry and range within the constraints of orbit design and mission operations. The SciBox functional structure is shown schematically in Figure 1.5. Because a pivot about the spacecraft–Sun line was incorporated into the MDIS design, the imaging observations could be planned with this additional degree of freedom not available to the other instruments. This capability motivated an altitude-based hierarchy of science pointing priority, by which different instruments were assigned attitude control for specific ranges of altitude. Attitude control was assigned to MLA for all altitudes less than the ranging limit (~1500 km) to the surface for a nadir point on the planet's nightside. Otherwise, pointing control was assigned to XRS on the dayside if the allowed range of directions of the spacecraft z-axis intercepted the planet. The remaining time in which the planet was within the MDIS field of regard was assigned to MDIS control, and the remainder of the observing time was assigned to exosphere observations by MASCS. The science team also identified prioritized sets of specific targets on the planet for focused observation (e.g., high resolution, additional colors, greater pointing dwell time). These targets were assembled into a target database and were selected if unsubscribed opportunities were present. Each instrument was also assigned an allocation for data volume, and a nominal plan for altitude-dependent data collection was designed for each of the instruments other than MDIS.

This database and the mission design were ingested to derive a draft observation plan and predictions for SSR loading for the entire orbital mission. The spacecraft orbit (in the form of kernels in the NASA Spacecraft, Planet, Instrument, C-matrix, Events – or SPICE – toolkit), times reserved for mission operations, and constraints on spacecraft attitude slew rate and MDIS pivot rotation rate (captured as rules) were used by the Opportunity Analyzer in SciBox to identify all possible imaging opportunities. The MDIS imaging plan was then constructed by the Opportunity Analyzer, which identified all achievable imaging opportunities given the spacecraft attitude as constrained by MLA- and XRS-assigned attitude and the MDIS pivot. These opportunities were next evaluated against the desired properties for imaging and requirements for imaging overlap by the Optimizer module, resulting in the generation of an imaging plan and a spacecraft science attitude

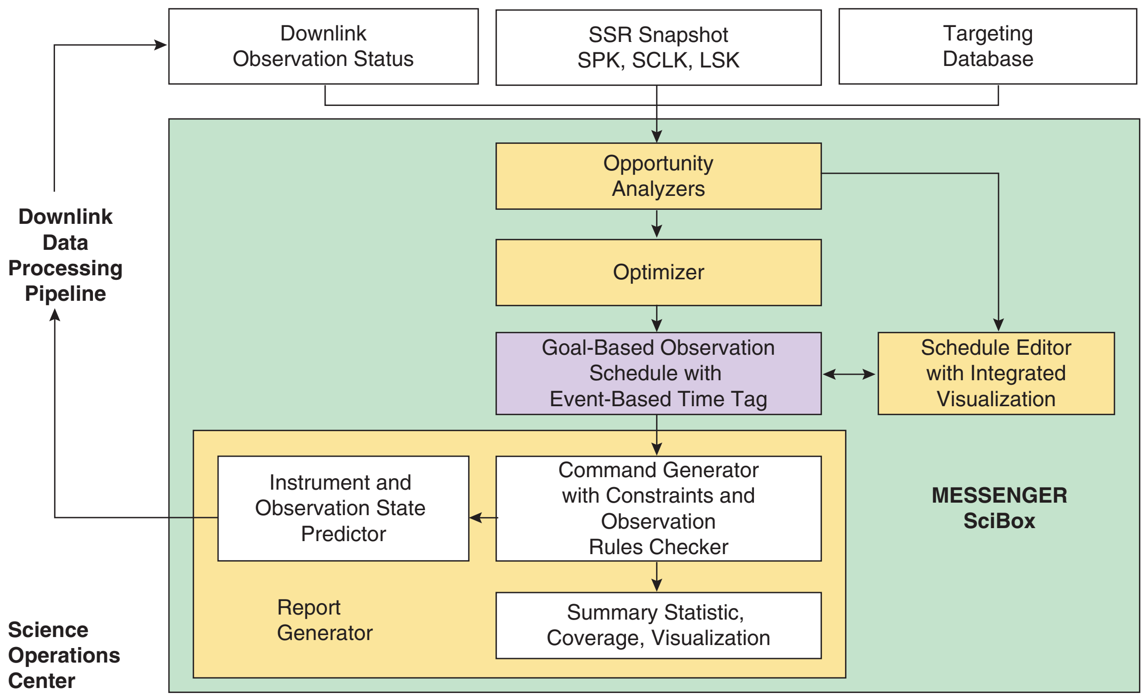

Figure 1.5. Functional schematic of the MESSENGER SciBox software suite (green box). Input data are indicated by white boxes at the top (downlink status, SSR data volume, attitude and orbit data in SPK, SCLK, and LSK SPICE kernels, and the targeting database); the main module elements are indicated by tan boxes; the key intermediate schedule product is indicated by the purple box; and key elements of the report generator are shown. The SciBox software was maintained and configured within the MESSENGER Science Operations Center, and the state predictor was used to update the SSR load predictions. SPK, SCLK, and LSK denote the Spacecraft and Planets Kernel, the Spacecraft Clock Kernel, and the Leapseconds Kernel, respectively.

plan. These plans were then checked against the spacecraft control constraints by the Rules Checker module, and draft spacecraft attitude and instrument commanding sequences were generated. The loading on the SSR was also evaluated and updated, including the expected downlink capacity for each communication pass. One key to ensuring accuracy of the planning against actual performance was that the times of commanding were keyed to orbit events rather than to absolute time. This procedure allowed the plan to transition smoothly from the orbit predictions far in the future to the immediate planned orbit using the latest orbit predictions to generate actual commands for the spacecraft.

The integrated plan was developed with an iterative approach by which successively more observations were included in the Opportunity Analyzer. Once it was demonstrated that the imaging goals could be met within the MLA and XRS constraints, the other pointed observations, including UVVS exosphere and surface targets, were included in the planning. In addition, the predictions for SSR loading were used to tailor the allowed instrument observation rates, and these revised data rates were included in refinements to the mission-long observation plan. Development and refinement of the modules continued throughout the orbital phase, including both extended missions, to track the additional science observation objectives.

1.3.4 Advance and Near-Term Science Planning

The integrated mission plan was used for both science planning and command generation (Berman et al., 2010). The plan was re-derived for each week of operations and updated with information acquired for imaging coverage, SSR loading, and any adjustments needed for instrument performance, operation, or spacecraft operations rules. This analysis constituted the Advance Science Planning process, which was the starting point for building the final command loads for the spacecraft. The command building process, known as Near-Term Science Planning, ran on a four-week cadence. A week's commands were generated four weeks ahead of execution on the spacecraft, and with each successive week the sequence was processed through different stages of review, quality assessment, and error checking. For actual spacecraft commanding, the SciBox suite included converters from the schedules to instrument operation and spacecraft attitude command requests in formats required by the mission operations scheduling and command-load development tools. These command requests were reviewed by the science and engineering teams for each instrument and then processed through the spacecraft command generator to verify compliance with all instrument and spacecraft rules. Each load was then run through the ground spacecraft simulator before being approved for upload and execution on the spacecraft.

1.3.5 Science Observation Performance

The performance of the observation planning during orbital operations resulted in imaging, mapping, and in situ surveys of the planet that met every project requirement for the